Version of Record: https://www.sciencedirect.com/science/article/pii/S0926337322008141
Manuscript_eda50ca52cd12b57b14f954c782d0152

Metathesis, Molecular Redistribution of Alkanes, and the Chemical Upgrading of Low-Density Polyethylene

Doyoung Kim[1,2], Zachary R. Hinton[1], Peng Bai[1,3], LaShanda T. J. Korley[1,2,4], Thomas H. Epps, III[1,2,4], and Raul F. Lobo[1,2,*]

[1]Center for Plastics Innovation, University of Delaware, Newark, Delaware 19716, United States

[2]Department of Chemical and Biomolecular Engineering, University of Delaware, Newark, Delaware 19716, United States

[3]Chemical Engineering Department, University of Massachusetts Amherst, Amherst, Massachusetts 01003-9303, United States

[4]Department of Materials Science and Engineering, University of Delaware, Newark, Delaware 19716, United States

*Corresponding author: lobo@udel.edu

© 2022 published by Elsevier. This manuscript is made available under the Elsevier user license
https://www.elsevier.com/open-access/userlicense/1.0/

Abstract

A new strategy for polyethylene (PE) deconstruction via alkane metathesis is presented, in which WO_x/SiO_2 catalyzes the olefin metathesis reaction step. Zeolite 4A is an essential component to protect the metathesis active sites from poisoning by in-situ-generated oxygenates in a batch reaction system. High conversion of 1-hexadecene (96%) and *n*-hexadecane (92%)—surrogates of long-chain molecules—demonstrates the high reactivity of WO_x/SiO_2 metathesis catalyst for olefin and alkane metathesis reactions, respectively, at moderate reaction temperatures of 300 °C for 2 to 3 h. Pretreatment temperature and length of the short *n*-alkane-chain solvent significantly affect the metathesis reactivity and selectivity. Results for the deconstruction of low-density PE (LDPE) in *n*-decane demonstrate a remarkable potential for PE upgrading with the advantages of short reaction times (3 h), the low mass ratio of solvent to LDPE, and the production of solid products with narrow molecular weight distributions.

Keywords

Alkane metathesis, molecular redistribution, chemical upgrading

1. Introduction

The negative environmental impact of plastic waste requires the urgent development of effective and economical plastic recycling and upgrading processes [1]. Polyethylene (PE) is the largest portion of the plastics waste stream and presents major challenges to chemical recycling due to the stability of the polymers' C-C bonds [2,3]. Numerous investigations utilizing various catalytic reactions for PE upgrading have been reported recently [4–17]. Catalytic alkane metathesis chemistry—comprising tandem (de)hydrogenation and olefin metathesis—has been explored as an alternative to direct deconstruction methods (*e.g.*, pyrolysis or hydrocracking) due to its moderate operating temperature (~200 °C) and absence of reactive gases (*i.e.*, H_2) in the process, two factors favorable for the economic viability of a metathesis-based chemical recycling process [18,19].

While alkane metathesis-based PE deconstruction has been demonstrated in the literature, the approach typically relies on a rhenium oxide catalyst for the olefin metathesis reaction [18,19]. Rhenium oxide is expensive, cannot be applied at the high temperatures at which reaction kinetics are most favorable (due to the high volatility of surface rhenium oxide species), and can be complex to regenerate [18–24]. We sought to substitute this catalyst with a silica-supported tungsten oxide (WO_x/SiO_2), a relatively inexpensive material that addresses the adverse features of rhenium oxide (cost ratio of rhenium/tungsten = 106 (w/w) [25]). Olefin metathesis [20,26-44] and alkane metathesis [45,46] using WO_x/SiO_2 have been applied in plug-flow reactor systems. They are generally known as molecular weight redistribution processes. However, there have been no reports of the application of this catalyst for either olefin or alkane metathesis reactions in a batch reactor system or for PE deconstruction. A batch reactor may be preferable to a flow reactor for PE upgrading to address the challenges of converting mixed plastics waste; therefore, understanding the conditions needed for catalyst operation in a closed system is key to developing successful upgrading processes.

A critical barrier to implementing closed-system alkane metathesis is the generation of aldehydes and ketones during catalyst activation because these species poison catalytic active sites—tungsten alkylidenes—on the surface of WO_x/SiO_2 [26,27,40,47]. Furthermore, given the molecular weight

redistribution features of alkane metathesis chemistry—which not only shortens but also lengthens the chains of the initial reactants—a thorough investigation of reaction variables, such as dilution ratio and catalyst pretreatment conditions, is needed to design processes that can control product distribution toward higher-value components. The development of a model reaction system that utilizes polymer surrogates to screen and optimize the most crucial reaction conditions must precede widespread adoption of polymer metathesis upgrading processes.

Herein, we develop model reactions of catalytic olefin and alkane metathesis using a WO_x/SiO_2 catalyst in a batch system. Using these model reactions, we evaluate the role of zeolite 4A (abbreviated 4A) adsorbent in facilitating catalyst activation and reaction in a closed/batch system. We assess the factors that affect the catalytic reactivity and selectivity of the system. We demonstrate that because WO_x/SiO_2 can operate in the range of temperatures inaccessible to rhenium oxide, shorter reaction times can produce high conversions of the surrogate reactant. Finally, we show that the reaction system described herein has significant potential for LDPE upgrading with remarkable efficiency gains in comparison to reports on the deconstruction of PE using catalytic metathesis via rhenium oxide [18,19]. To the best of our knowledge, this report is the first study in which WO_x/SiO_2 has been successfully implemented in the closed-batch reactor and, specifically, for the chemical upgrading of PE.

2. Experimental

Please see **Appendix** for the list of acronyms and abbreviations.

2.1. Catalyst synthesis

WO_x/SiO_2 (2 wt%) was prepared by wet impregnation. 6.4 g of 4.7 mM ammonium meta-tungstate hydrate ($(NH_4)_6H_2W_{12}O_{40}\cdot xH_2O$, 99.99%; Sigma Aldrich) precursor solution was added dropwise to 4.0 g of a silica support (SiO_2; Davisil, Grade 643; Sigma Aldrich) and mixed using a spatula for 12 min. The mixture was dried under static air at 120 °C for 24 h in an oven. Finally, the dried mixture was transferred to a tube furnace at 120 °C for 2 h and then calcined at 500 °C for 12 h with a ramp rate of 3 °C/min in a 1000 mL/min flow of air.

Zeolite 4A (beads, 8-12 mesh) was purchased from Sigma Aldrich and activated by heating from ambient temperature (~23 °C) to 310 °C (1 °C/min) and then holding at 310 °C for 15 h under airflow (200 mL/min) in a muffle furnace. The activated 4A was stored in an airtight container before use. Pt/γ-Al_2O_3 (1 wt%, abbreviated PA) was purchased from Alfa-Aesar and used as received.

2.2. Catalyst characterization

The X-ray diffraction (XRD) patterns of samples were collected using a Brucker D8 diffractometer in θ-θ geometry with a step size of 0.03° and a 1 s scan per point. The catalyst surface area and pore volume were measured by N_2 adsorption-desorption experiments at 77 K using a 3Flex surface characterization analyzer (Micrometrics) after the samples were pretreated at 300 °C for 6 h under vacuum. Elemental analysis via X-ray fluorescence (XRF) was conducted using a Rigaku wavelength dispersive XRF (WDXRF) instrument. Carbon monoxide chemisorption was performed using the pulse technique on a Micromeritics AutoChem II. Images of the surface morphology of the samples were obtained with a scanning electron microscope (SEM, Auriga-60, ZEISS) using 3.00 kV accelerating voltage. Prior to the SEM experiments, the samples were coated with gold/palladium alloy. The Raman spectrum of catalyst powder was collected by a Horiba LabRam microscope using a 325 nm UV-laser with a 15x objective.

2.3. Model reactions of catalytic olefin and alkane metathesis

For the olefin metathesis model reaction, the metathesis of 1.56 g of 1-hexadecene (>99.0%; TCI America) was carried out in *n*-heptane (99%; Fisher Chemical) at a molar ratio of 9.8:1 (*n*-heptane:1-hexadecene). A total of 0.8 g of WO_x/SiO_2 and 1.0 g of 4A were added to the reactor as olefin metathesis catalyst and adsorbent, respectively. This model reaction is denoted olefin-metathesis (C7/C16).

The alkane metathesis model reaction was carried out using 1.58 g of *n*-hexadecane (99%, anhydrous; Acros Organics) and the corresponding amount of short-chain alkane, either *n*-heptane or *n*-decane (>99.0%; TCI America), at a molar ratio of 9.8:1 (short-chain alkane:*n*-hexadecane). These model reactions are named alkane-metathesis (C7/C16) and alkane-metathesis (C10/C16), respectively. For alkane metathesis of PE, 1.55 g of LDPE (M_w ~ 75 kDa; Sigma Aldrich) and 9.7 g of *n*-decane were used, and the model reaction was denoted alkane-metathesis (C10/LDPE). For all alkane metathesis reactions,

0.5 g of PA was used as a (de)hydrogenation catalyst together with the same amount of WO_x/nd 4A as used for the olefin-metathesis (C7/C16).

All the liquid reactants for each experiment were mixed using a magnetic stirrer and dehydrated using the activated 4A in an airtight glass bottle at room temperature for 2 h prior to the reaction. Plastic pellets of LDPE were used as received without any further mechanical treatment (*e.g.,* grinding).

2.4. Catalyst pretreatment and reactivity tests

Catalyst pretreatment and the metathesis reactions were performed as follows: catalysts and adsorbent were placed into a 50-mL, stainless-steel, pressure reactor (Parr) and mechanically mixed by a spatula prior to closing the reactor. The pretreatment consisted of dehydrating this mixture under 100 mL/min flow of helium at the desired temperature (450 or 480 °C) for 2 h, including a ramping period (10 °C/min). Helium (Grade 5.0; Keen Compressed Gas Co.) was purified by oxygen/moisture traps (Restek) and then flowed through the reactor continuously. After this period, the reactor was cooled to room temperature using an ice bath. The liquid feedstock, corresponding to each specific reaction, was added to the reactor using a glass syringe connected to the reactor via a Luer-to-threaded NPT connector (**Figure S1**) to avoid exposing the pretreated catalyst to oxygen.

For the case of alkane-metathesis (C10/LDPE), the desired mass of plastic pellets was added via a ball valve after adding the liquid mixture. The reactor was continuously purged with a flow of 100 mL/min of dry He. This procedure ensured that minimal air or water vapor contaminated the interior of the reactor when the pellets were introduced. After adding all reactants, the reactor was purged ten times with N_2 (up to 5 bar) to remove any residual oxygenates in the vessel and ensure all liquid was in the bottom of the reactor. Finally, the reactor was charged to 30 bar of N_2 at room temperature and heated to a reaction temperature of 300 °C (at a 10 °C/min ramp rate) while stirring with a magnetically driven impeller at 800 rpm. The reaction time in **section 3** includes the temperature ramping period (~30-40 min). The reactor was quenched by an ice bath at the specified reaction time. A schematic of the procedure is shown in **Figure S2**.

2.5. Product analysis

Gas products in the headspace of the reactor were transferred to a Tedlar gas sampling bag and analyzed with a gas chromatography-flame ionization detector (GC-FID) (Agilent HP-Plot GC column). Products of carbon numbers between 1 and 8 in the gas phase were detected with GC-FID by Tedlar sampling bags filled with samples from the reactor headspace, and the yields of these products were calculated based on the ideal gas law and calibration curves measured with standards. The mixture of liquid products, catalysts, adsorbents, and wax remaining in the vessel was then collected in a beaker. The reactor was rinsed with 50 mL of CH_2Cl_2 (HPLC grade, Fisher Chemical), and this solution was mixed with the recovered reactor contents. 0.2 g of mesitylene (99%, Extra Pure; Acros Organics) was added to the collected products as an internal standard. This mixture was separated by filtration (11 μm; GE Whatman), yielding a liquid filtrate and solid residues. The liquid was analyzed by GC-FID (Agilent HP-1 column) and gas chromatography-mass spectrometry (GC-MS) (Agilent DB-1 column). For GC-FID measurements, the temperatures of the inlet and FID detector were maintained at 300 °C, and the oven was started at 40 °C, held for 5 min, ramped to 300 °C (at 15 °C/min), and then held for 5 min. The conversion of each feedstock was calculated as

$$Conversion\ (\%) = \frac{n_{final}}{n_{initial}} \times 100$$

in which $n_{initial}$ is the total number of moles of carbon atoms in the initial feedstock, and n_{final} is the total number of moles of carbon atoms in the remaining after the reaction. The moles of feedstock (*i.e.*, *n*-heptane, *n*-decane, *n*-hexadecane) consumed by each reaction was calculated using a material balance given the starting and final quantities (the latter of which was measured via GC-FID). A correction was made to account for losses of feedstock due to the addition of reactants to or collection of products from the reactor. A control experiment was performed in which: (1) feedstock in the same quantity used for the model reactions was added to the empty reactor via the syringe (see **section 2.4**), (2) the reactor was purged five times under 5 bar of N_2, (3) the feedstock was collected in a beaker by rising the reactor with 50 mL of CH_2Cl_2, and (4) the solution was analyzed by GC-FID after the addition of 0.2 g of mesitylene to the sample. The typical loss of *n*-heptane was ~5% whereas that of *n*-decane and *n*-hexadecane was <1%

for each. Based on these results, 5% was added to n_{final} for the calculation of conversion with respect to *n*-heptane. The yield and selectivity of the products with carbon number *i* were calculated by following equations:

$$Y_i\ (\%) = \frac{n_i}{n_{long,\ initial}} \times 100;\ S_i\ (\%) = \frac{n_i}{\sum n_j} \times 100$$

in which n_i is the total number of moles of carbon atoms in the product species with carbon number *i*, $n_{long,\ initial}$ is the total number of moles of carbon atoms in the long-chain alkane or alkene reactant corresponding to each model reaction (*e.g.*, $n_{long,\ initial}$ is the total number of moles of carbon atoms in initial 1-$C_{16=}$ for olefin-metathesis (C7/C16)), and $\sum n_j$ indicates the total yield of products in the liquid mixture (*i.e.,* excluding wax). For products of carbon numbers ranging between 5 and 15, *n*-alkanes corresponding to each carbon number were used to determine the calibration factors (*i.e.*, by correlation of known concentration). The effective carbon numbers of products greater than 15 were set equal to that of the internal standard.

The yields of species of carbon number 3 - 8 were included in the total yield of liquid products because most of these hydrocarbons were condensed or dissolved, rather than transferred to the gas sampling bag after the reaction. The yield and selectivity of gas products of carbon number <3 are not represented below because they were only present in small quantities (< 0.05% recovered). The carbon balance (C.B.) of reactions was calculated as

$$C.B.\ (\%) = \frac{\sum n_j + n_{wax}}{n_{short,\ initial} + n_{long,\ initial}} \times 100;\ n_{wax} = \frac{2 \times w_{wax}}{28}$$

in which $n_{short,\ initial}$ is the number of carbon atoms in the alkane feedstock of short-chain length, n_{wax} is the number of carbon atoms in the wax product, and w_{wax} is the mass of wax. Some of the liquid compounds are likely adsorbed on 4A, causing a reduction in the total C.B. of reactions; however, quantification of these products was not performed.

The solid residues from the product mixture were analyzed by high-temperature gel permeation chromatography (HT-GPC) in the cases in which a solid product was recovered. To this end, an aliquot of

the residue was dissolved in toluene at 100 °C, and the clear solution was decanted to remove catalyst and adsorbent particles. We have previously demonstrated that this method adequately separates all residues from the catalyst-residue mixture with high reproducibility (i.e., multiple random samples yield the same product distribution [4]). The solutions were then dried completely using a rotary evaporator and prepared for HT-GPC by dissolving 1.5 mg/mL in the mobile phase at 140 °C for approximately 3 h. HT-GPC was performed using a high-temperature chromatograph (Tosoh HLC-8312GPC/HT), with two TSKgel GMHHR-H(20)HT and one TSKgel D2000HHR(20) columns in series. The mobile phase, 1,2,4-trichlorobenzene (HPLC grade; Fisher Chemical) with 500 ppm butylated hydroxytoluene (Fisher Chemical), was maintained at 140 °C and a flowrate of 0.8 mL/min for a total elution time of 80 min. Molecular weights were determined using calibration runs of 13 narrow polystyrene standards in the range of $5x10^2$ to $2x10^6$ Da with molecular weight values of the solid samples adjusted by the Mark-Houwink constants for polystyrene and PE [48]. The resulting Mark-Houwink-corrected molecular weight range for PE samples was $8x10^1$ to $6x10^5$ Da. The weight (M_w) and number (M_n) average molecular weights were determined by discrete integration (using standard methods [48]) of the distributions obtained from the refractive index (RI) detector response, including only data corresponding to Mark-Houwink-corrected molar masses greater than $3x10^2$ Da.

3. Results and discussion

3.1. Characterization of the catalysts

Given that the surface-isolated tungsten alkylidene species are the active sites for heterogeneous olefin metathesis [20,26,27,49,50], the loading of W was set to 2 wt% to minimize waste metal when synthesizing catalyst. The Raman spectrum (**Figure S3**) of a WO_x/SiO_2 olefin metathesis catalyst revealed that tungsten oxide was present in dehydrated monomeric form with peaks at 905, 985, and 1015 cm^{-1} [51-53]. Raman features for bulk WO_3 nanoparticles (270, 720, and 805 cm^{-1}) and the diffraction peaks for monoclinic crystalline tungsten oxide were absent in the XRD pattern (**Figure S4(a)**) [26,27]. Additionally, minimal change in the Brunauer–Emmett–Teller (BET) surface area (S_{BET}) and pore volume (V_p) of the silica support after synthesizing WO_x/SiO_2 was measured, indicating that the tungsten

oxide species was well-dispersed rather than blocking the pores of the silica support (**Table 1** and **Figure S4(b)**).

SEM images of WO_x/SiO_2 and PA illustrate the morphology and approximate particle size distribution of the catalyst samples (**Figure 1**). While WO_x/SiO_2 catalyst had a spherical shape and broad distribution of particle sizes, PA was obtained as platelets with flat surfaces and a narrower particle size range.

Table 1. Physical and chemical properties of the catalysts

Sample	S_{BET} (m^2/g)	V_p (cm^3/g)	Metal loading (wt%)[a]	Pt size (nm)[b]
SiO_2	279	1.1	-	-
WO_x/SiO_2	271	1.1	2.0[c]	-
PA	156	0.5	1.0	1.1

a: Determined by XRF
b: Determined by CO chemisorption
c: Metal loading was calculated based on WO_3

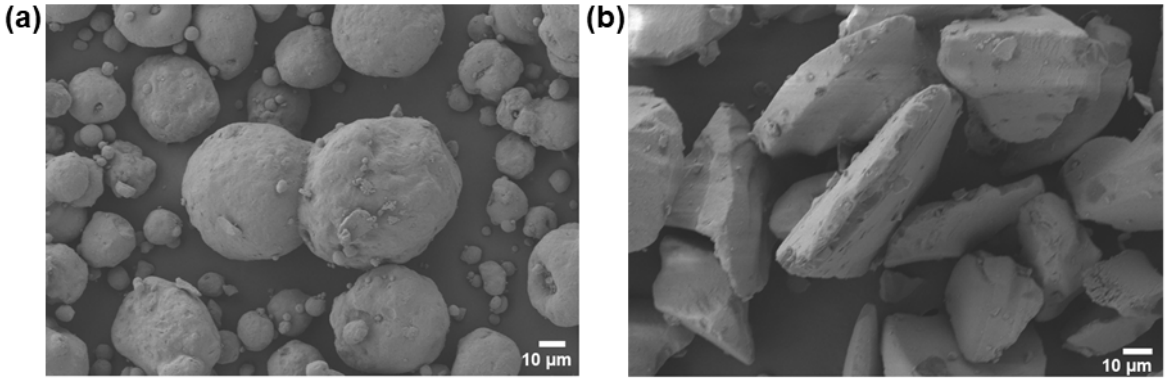

Figure 1. SEM image of (a) WO_x/SiO_2 and (b) PA.

3.2. Activation of WO_x/SiO_2 with 4A in closed batch system: olefin-metathesis (C7/C16)

The objectives of the olefin-metathesis (C7/C16) reaction were to establish the operating conditions under which WO_x/SiO_2 catalyst can be effectively activated in the batch reactor and to evaluate the catalytic reactivity of WO_x/SiO_2 for the molecular redistribution of a long alkene (1-hexadecene). The WO_x/SiO_2

pre-catalyst surface species—surface-isolated tungsten di/mono-oxo compounds—need to be reduced and re-oxidized by the olefin to generate the surface-active sites—tungsten alkylidene—prior to the catalytic reaction. This process leads to the formation of aldehydes or ketones; *e.g.,* acetone is typically produced during the propylene metathesis reaction [26-28,54]. Though tungsten oxide species are easily poisoned by oxygenates, deactivation can be circumvented in a plug flow reactor because the fluid constantly removes oxygenate intermediates and hydrocarbon products from the catalyst surface. In a closed system, contact between the oxygenates and the catalytic tungsten oxide species is unavoidable. Therefore, we sought an alternative by which these detrimental oxygenates can be separated from the catalytic sites, preventing poisoning. Zeolite 4A was chosen because it is widely available and strongly adsorbs polar species (*e.g.,* water, alcohols, aldehydes, and ketones), which are produced during the activation process and during the hydrogenation of intermediates. Additional experiments demonstrated a ~20-30 wt% reduction in oxygenate concentration (**Table S1**). The essential advantages of 4A during activation and reaction were verified by comparing the results of olefin metathesis of C7/C16 mixtures to those from control experiments conducted with WO_x/SiO_2 in the absence of 4A. Experiments performed with 4A produced a wide distribution of olefin compounds (**Figure S5**); however, the control experiments generated no such products (*i.e.,* only unidentified compounds, not shown). Though the adsorption capacity of 4A at the operating temperature (300 °C) is expected to be small [55,56], enough of the in-situ-generated oxygenates during activation in the closed system are removed, and activated-WO_x/SiO_2 is prevented from deactivation prior to olefin metathesis.

Under the reaction conditions in which 4A was investigated, high conversion (~96%) of 1-$C_{16=}$ was achieved, resulting in a broad distribution of products of different carbon numbers (C_3 – C_{35}). This product distribution aligns well with the high catalytic reactivity of WO_x/SiO_2 with respect to the molecular redistribution process (**Figure S5, red traces** and **Table 2, entry 1**). Three hydrocarbon species are identified for each carbon number (3 - 35), corresponding to *α*-olefins, olefin isomers, and *n*-alkanes. The formation of the olefin isomers was expected due to well-known olefin isomerization side reactions in WO_x/SiO_2-catalyzed olefin metathesis [27,28,35,36]; however, *n*-alkanes also were produced in the absence of a (de)hydrogenation catalyst (**Figure S5**). Considering that (de)hydrogenation reactivity via the partially reduced tungsten oxide catalyst (WO_{3-x}) has been reported [29,57,58], the production of *n*-

alkanes may be the result of (de)hydrogenation reactions catalyzed by WO_{3-x} species of WO_x/SiO_2. The hydrogen for *n*-alkane formation was likely supplied by dehydrogenation of olefin intermediates or the abundant *n*-C_7 solvent. Further dehydrogenation of these intermediates may lead to the formation of coke precursors (**Figure S6(a)**). The pale-yellow color of the product solution (**Figure S7(a)**), low conversion of *n*-C_7 (6%), and formation of heptenes also support this hypothesis. *n*-Heptenes were detected by GC-MS but were difficult to quantify due to their overlap with *n*-heptane peaks.

Table 2. Results for olefin/alkane metathesis reactions

Entry	Metathesis reaction	Catalyst (mass, g)	Catalyst pretreatment temperature (°C)	Reaction time (h)	Conversion		Yield		CB (%)
					Short-chain alkane (%)	Long-chain alkane/olefin (%)	Liquid (%)[a]	Solid (g)[b]	
1	Olefin-metathesis (C7/C16)	WO_x/SiO_2 (0.8) 4A (1.0)	450	2	6.0 (3.3)[c]	96.4 (1.6)[c]	77.7 (1.5)[c]	N/A	92.2 (2.6)[c]
2	Alkane-metathesis (C7/C16)	WO_x/SiO_2 (0.8) PA (0.5) 4A (1.0)	450	2	28.3 (7.0)[c]	87.7 (3.0)[c]	164.8 (22.0)[c]	N/A	92.6 (1.9)[c]
3			480	1	15.8[d]	64.9[d]	107.3[d]	N/A	95.9[d]
4				2	57.4 (1.4)[c]	91.6 (0.3)[c]	252.4 (9.6)[c]	0.3 (0.0)[c]	88.9 (1.4)[c]
5	Alkane-metathesis (C10/C16)		480	1	10.8[d]	19.1[d]	77.6[d]	N/A	99.3[d]
6				2	48.0 (2.3)[e]	57.6 (1.4)[e]	316.6 (25.8)[e]	N/A	96.5 (1.6)[e]
7				3	81.6 (2.7)[f]	74.8 (2.8)[f]	448.3 (32.6)[f]	0.8 (0.4)[f]	93.9 (3.3)[f]
8	Alkane-metathesis (C10/LDPE)			3	60.2 (3.6)[e]	N/A	349.5 (18.9)[e]	1.0 (0.0)[e]	95.4 (0.3)[e]

Operating temperature of all reactions, 300 °C; for olefin-metathesis, 1-$C_{16=}$ of 1.56 g (*n*-C_7/1-$C_{16=}$ = 9.8 (mol/mol) added; for alkane-metathesis using C16 surrogate molecule, *n*-C_{16} of 1.58 g (*n*-$C_{7\text{ or }10}$/*n*-C_{16} = 9.8 (mol/mol)) added, and when using LDPE, LDPE (M_w ~75 kDa) of 1.55 g (*n*-C_{10}/LDPE = 6.3 (g/g)) added.

[a]: This value is calculated on a long-chain alkane/olefin (*i.e.,* 1-$C_{16=}$, *n*-C_{16}, and LDPE) basis

[b]: Mass of dried solid residual excluding the mass of the initial catalysts and adsorbent

[c]: Average and standard deviation of reaction quadruplicates

[d]: Single reaction result

[e]: Average and half range of reaction duplicates

[f]: Average and standard deviation of reaction triplicates

It should be noted that migration of W from WO_x/SiO_2 to 4A may have occurred during the catalyst pretreatment. This migration of elemental W was confirmed by a scanning electron microscope with energy dispersive X-ray spectrometer (SEM-EDX) with a measured concentration of ~0.1-0.2 wt% (standard deviation of 0.1) on 4A. However, the catalytic impact of tungsten in 4A is likely negligible because of the internal diffusion limitation within micropores (~4 Å diameter) of 4A that would hamper the rate of the olefin metathesis reaction.

3.3 Application of WO_x/SiO_2 to alkane-metathesis and alkane cross-metathesis (C7/C16)

High conversions of reactants (*n*-C_7 and *n*-C_{16}) and characteristic molecular redistribution of the metathesis reaction also were achieved using WO_x/SiO_2 for alkane-metathesis (C7/C16) under reaction conditions identical to those of the corresponding olefin-metathesis (C7/C16) (except the substitution of 1-$C_{16=}$ with *n*-C_{16}) (**Figure 2(a)** and **Table 2, entry 2**). Although the Pt-catalyzed, non-oxidative dehydrogenation of alkanes typically requires high operating temperatures (~500-600 °C) to achieve a satisfactory yield of the targeted alkene due to the high endothermicity of the reaction [59], the reaction conditions (*e.g.,* loading of Pt catalyst and operating temperature) for our tandem catalysis reaction generate sufficient olefin intermediates for the olefin metathesis step to proceed, giving rise to high conversions of both alkane reactants. The turnover numbers (TON) for Pt and W were 984 and 364, respectively (**Table 2, entry 2**). These values confirm that the reaction was catalytic. Note that the tungsten-based TON is an under-estimate because all tungsten atoms were assumed to be active sites for olefin metathesis. Control experiments conducted without PA (blank, with only WO_x/SiO_2, and with both WO_x/SiO_2 and 4A) yielded conversions below 5 % of each alkane reactant, whereas an experiment conducted with only PA showed conversion of 7 % and 36 % for *n*-C_7 and *n*-C_{16}, respectively. These relatively high conversions were attributed to the cracking properties of PA. Compared to the original experiment (**Table 2, entry 2**), these results support that each solid component is necessary to unlock the catalytic tandem reaction. Overall, these results indicate that WO_x/SiO_2 can be activated appropriately to catalyze the olefin metathesis stage of the entire tandem cycle in the closed batch reactor with the aid of 4A.

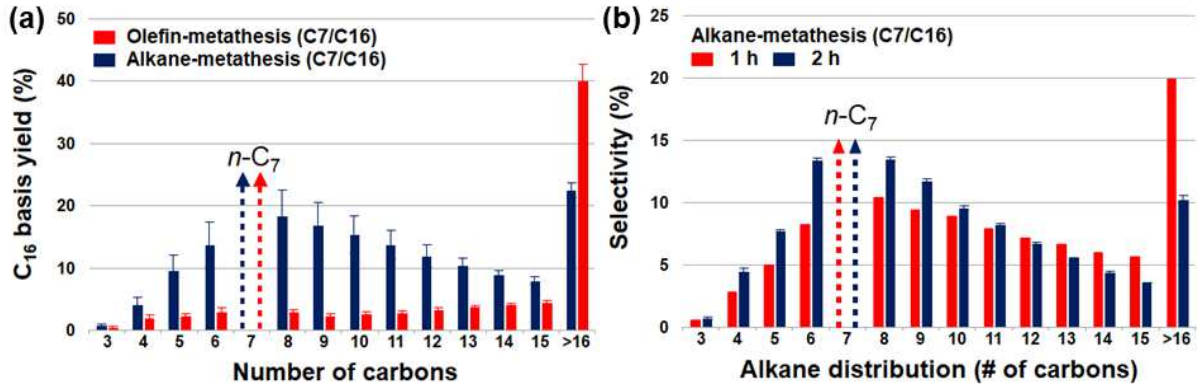

Figure 2. (a) Yield of liquid products of different carbon number. For olefin-metathesis (C7/C16), 1-$C_{16=}$,1.56 g (*n*-C_7/1-$C_{16=}$ = 9.8 (mol/mol)); WO_x/SiO_2, 800 mg; 4A, 1.0 g. For alkane-metathesis (C7/C16), *n*-C_{16}, 1.58 g (*n*-C_7/*n*-C_{16} = 9.8 (mol/mol)); PA, 500 mg; WO_x/SiO_2, 800 mg; 4A, 1.0 g. Pretreatment conditions: 450 °C; He flow (100 mL/min); 2 h. Reaction conditions: 300 °C; N_2, 30 bar; 2 h. Data for the added alkane reagent/solvent in (a) were omitted. The bars represent an average of reaction triplicates with error bars indicating a standard deviation. (b) Product selectivity of alkane compounds in the liquid products of alkane-metathesis (C7/C16) at different reaction times; 1 h and 2 h. *n*-C_{16}, 1.58 g (*n*-C_7/*n*-C_{16} = 9.8 (mol/mol)); PA, 500 mg; WO_x/SiO_2, 800 mg; 4A, 1.0 g. Pretreatment conditions: 480 °C; He flow (100 mL/min); 2 h. Reaction conditions: 300 °C; N_2, 30 bar. The bars represent the result of a single reaction for the 1 h case and an average of quadruplicates with error bars indicating a standard deviation for the 2 h case. Data for the added alkane reagent/solvent in (a) and (b) were omitted.

Alkane cross-metathesis—the reaction between short- and long-chain alkanes—is the desired reaction because incorporating the short-chain into the long-chain leads to a rapid reduction of the effective length of the polymer toward the products of interest. Whether efficient molecular redistribution of LDPE surrogate (*n*-C_{16}) would occur via the cross-metathesis was determined by comparing the trends of the product yields of olefin-metathesis and alkane-metathesis (C7/C16) reactions. While the conversions of C_{16} reactants of these model reactions differ by only 10%, the C_{16} basis yield for compounds with carbon numbers greater than 16 is double for olefin-metathesis (C7/C16) in comparison to that of alkane-metathesis (C7/C16) (**Figure 2(a)**). This result suggests that carbon atoms originating from *n*-C_7 were effectively incorporated into the compounds of carbon number greater than 16, indicating that the product selectivity towards alkanes smaller than carbon number 16 for alkane-metathesis (C7/C16) becomes greater than that of olefin-metathesis (C7/C16).

The effect of pretreatment temperature was investigated by performing separate alkane-metathesis (C7/C16) reactions after dehydration of catalyst substrates at 450 and 480 °C. A higher pretreatment

temperature increased the consumption rate of both *n*-C_7 and *n*-C_{16}, with a greater enhancement measured for *n*-C_7. As a result, product yields increased by ~50%, although the carbon balance was reduced from 93% to 89%. The conversion of *n*-C_7 for entry 2 (**Table 2**) decreased by approximately half when 4A was used without the separate ex-situ activation at 310 °C before catalyst pretreatment (**Method 2.1**). This reduced activity presumably was due to the 4A not being completely dry, even after the pretreatment, leading to a reduction in the ability to scavenge the oxygenates generated during the activation process and diminishing the ultimate number of active sites on WO_x/SiO_2. Alternatively, after pretreatment, the incompletely dehydrated 4A desorbed a small quantity of water, deactivating the active sites.

By increasing the pretreatment temperature, reaction rates are expected to be enhanced by further dehydrating the sample toward an improvement in the overall conversion of reactants and an increase in product yields. Care must be taken to maximize pretreatment temperatures without inducing structural damage to the catalyst or adsorbent. A reduction in the carbon balance can partly be explained by the production of coke-related species (**Figure S6(a)** and **(b)**), as indicated by the darker yellow color of the product solution of entry 4 in comparison to other entries (**Figure S7(a)** and **Table 2**). Interestingly, the solution prepared for HT-GPC of the solid residuals from entry 4 (separated from the catalysts and 4A) contained insoluble, microscopic particles that had to be filtered out from the solution. Even after filtration, the solution remained clear with a brown color, suggesting the presence of potential coke-like precursors (possibly polycyclic aromatic species).

The effect of reaction time on the catalytic reactivity was investigated by running the alkane-metathesis (C7/C16) reactions for 1 h and 2 h after the pretreatment at 480 °C. The Pt-based TON increased from 592 to 1763 after 1 h (**Table 2, entries 3** and **4**). The approximately 3x-lower TON at 1 h could be not only due to the inclusion of the temperature ramping period (~ 30-40 min), but also to an induction period during which the surface WO_x species are activated [49,57]. Additionally, it can be observed that the selectivity towards C16+ alkanes decreased as the reaction time increased (**Figure 2(b)**) (see below).

3.4 Effect of the short alkane length in alkane-metathesis (C10/C16)

PE solubility is highly dependent upon the choice of organic solvent, which ultimately affects catalytic deconstruction rates via factors such as heat/mass transfer and the nature of substrate-catalyst interaction. Even chemically similar, non-polar, organic solvents (*e.g.*, *n*-pentane and *n*-hexane) can display different performance characteristics in the catalytic deconstruction of PE based on dissimilarities in polymer solubility and conformation at the reaction temperature [8,60,61]. We performed alkane-metathesis (C10/C16) to investigate the effect of the length of the short alkane species on the molecular redistribution of PE surrogate, *n*-C_{16}, by replacing *n*-C_7 (T_c = 267.46 °C) with *n*-C_{10} (T_c = 344.65 °C) [62]. Considering the reaction temperature (300 °C), one noticeable difference between alkane-metathesis (C7/C16) and alkane-metathesis (C10/C16) is the thermodynamic state of the shorter length alkanes (*i.e.*, C_7 and C_{10}): supercritical fluid and liquid, respectively. Reaction time (1 - 3 h) was adjusted~~,~~ but other reaction parameters (*e.g.,* pretreatment temperature, reactant molar ratio, catalyst loading, nitrogen pressure, *etc.*) were kept constant.

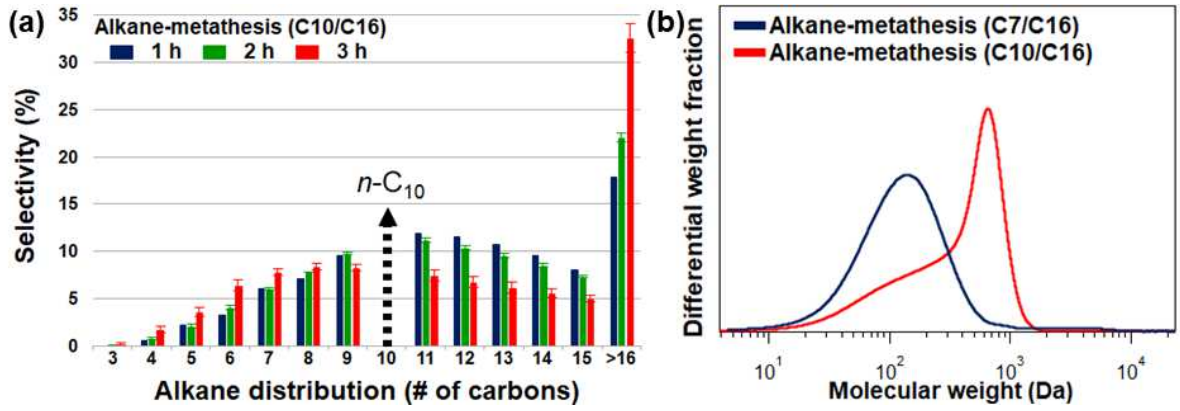

Figure 3. (a) Product selectivity of alkane compounds in the liquid products of alkane-metathesis (C10/C16) at 1 h, 2 h, and 3 h. *n*-C_{16}, 1.58 g (*n*-C_{10}/*n*-C_{16} = 9.8 (mol/mol)); PA, 500 mg; WO_x/SiO_2, 800 mg; 4A, 1.0 g. Pretreatment conditions: 480 °C; He flow (100 mL/min); 2 h. Reaction conditions: 300 °C; N_2, 30 bar. Single reaction result for 1 h measurement and averages of duplicates and triplicates with error bars indicating the half of range and standard deviation for the 2 h and 3 h measurements, respectively. Data for the added alkane reagent/solvent in (a) were omitted. (b) Differential molecular weight distributions of the post-reaction solid residues from alkane-metathesis (C7/C16), 2h; alkane-metathesis (C10/C16), 3 h (as measured by HT-GPC).

The Pt-based TONs for alkane-metathesis (C10/C16) were 337 and 1423 after 1 h and 2 h of reaction time, respectively (**Table 2, entries 5** and **6**), and demonstrated that the reaction remained catalytic. In comparison to alkane-metathesis (C7/C16) (**Table 2, entries 3** and **4**), the overall rate was slower for the

first two hours; however, the relative rate (*i.e.*, the ratio of the number of converted short alkane to that of C16, r_{short}/r_{16}) increased from 2.4 to 6.1 and from 5.5 to 8.2 for the 1 h and 2 h reactions, respectively, after replacing *n*-C_7 with *n*-C_{10}.The higher relative rates for alkane-metathesis (C10/C16) indicate that *n*-C_{10} reacted more frequently (relative to *n*-C_{16}) in the reaction than *n*-C_7. This difference can be attributed not only to the different phase behaviors of the short alkane species on the rate, but also to the effects of the different substrate lengths on adsorption and to the intrinsic rate of either dehydrogenation or olefin metathesis [50,63]. When comparing entries 4 and 7 (**Table 2**), the relatively increased reactivity for *n*-C_{10} led to a decrease in *n*-C_{16} conversion by ~20%.

The use of *n*-C_{10} as the short alkane: (*i)* shifted to the liquid product selectivity towards higher molecular weight alkanes (>C16) as time increased (**Figure 3(a)**) in contrast to the results for *n*-C_7 (**Figure 2(b)**), (*ii)* resulted in the formation of higher molecular weight wax (**Figure 3(b)** and **S8(a)**), and (*iii)* reduced coke precursor formation, as demonstrated by a change in the optical properties of the product (**Figure S6(a)** and **S7(b)**) and improved carbon balance (**Table 2, entries 5-7**). Unlike other catalytic chemistries for PE chemical recycling (hydrocracking, hydrogenolysis, pyrolysis, *etc.*) that mainly lead to a reduction in molecular weight, alkane metathesis can produce both lower and higher molecular weight compounds (with respect to initial reactants) simultaneously. The molar fraction of the short alkane (*n*-C_{10} here) that was incorporated into longer chains in the final product was greater than 40% in comparison to *n*-C_7 (**Table 2, entries 4** and **7**). Higher degrees of incorporation of small alkanes into longer chains could be related to the solubility of wax and oligomer intermediates in the reaction media, namely supercritical *n*-C_7 versus liquid *n*-C_{10}. Jia *et al.* postulated that the higher hydrogenolysis reactivity for HDPE in liquid *n*-hexane than that in supercritical *n*-pentane could be attributed to the higher solubility of PE in the former versus the latter [8]. The high solubility of waxy intermediates/products generated in the liquid phase of *n*-C_{10} during alkane-metathesis (C10/C16) experiments might facilitate the continued growth of wax molecular weights as the reaction proceeds. The solid products have two overlapping peaks in the molecular weight distribution: one centered around ~100 Da, corresponding to mid-length hydrocarbons, and another around ~700 Da, corresponding to light wax (**Figure 3(b)**). In the case of alkane-metathesis (C7/C16), the solid products are primarily composed of broad molecular weight, mid-length hydrocarbons

with a negligible amount of light wax (**Figure 3(b)**). These results agree with the lower solubility of longer alkanes in *n*-C_7 during the reaction, leading to insolubility before sufficient wax can be generated.

3.5. LDPE chemical upgrading using *n*-C_{10} as short length alkane: alkane-metathesis (C10/LDPE)

The effectiveness of this catalytic molecular redistribution reaction system for the chemical upgrading of LDPE was verified using virgin LDPE (M_w ~ 75 kDa). Although the same mass of LDPE as *n*-C_{16} for alkane-metathesis (C10/C16) was used for the reaction, the conversion of *n*-C_{10} decreased by about 30% for the alkane-metathesis (C10/LDPE) in comparison to that of alkane-metathesis (C10/C16) (**Table 2, entries 7** and **8**). The lower conversion might be attributed to the decreased diffusion rate in the bulk and lower coverage by *n*-C_{10} on the catalyst surface caused by higher viscosity and wetting of the catalyst contributed by the polymer chains [4,13,60,64]. As a result, the yield of liquid products for alkane-metathesis (C10/LDPE) was reduced by 20% in comparison to alkane-metathesis (C10/C16), whereas product selectivity remained similar (**Figure 4(a)**). The solid yield increased by 25% (**Table 2, entries 7 and 8**) because the initial length of the LDPE was much longer than *n*-C_{16}, leading to higher molecular weight products. Note that the solid residues are not of higher yield because of unreacted polymer, which is not measured in the molecular weight distribution of the product.

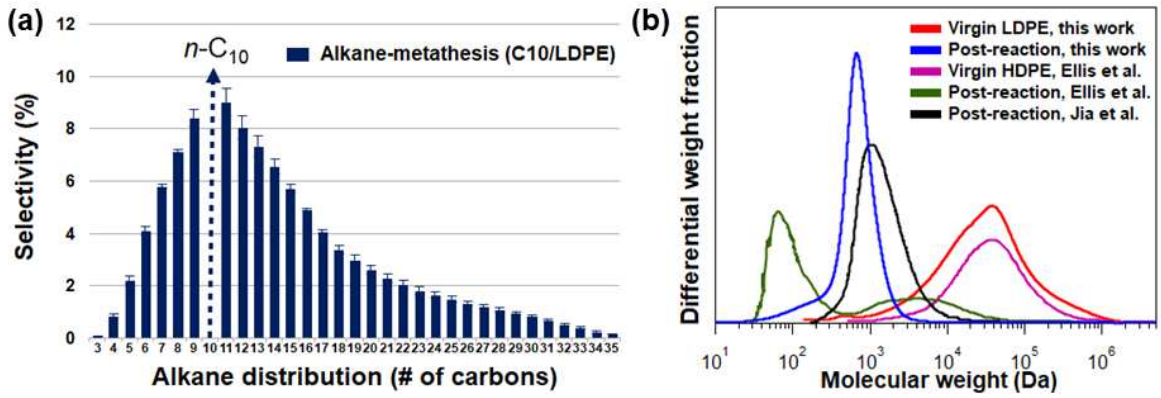

Figure 4. (a) Product selectivity of alkane compounds of liquid products for alkane-metathesis (C10/LDPE). LDPE (M_w ~75 kDa), 1.55 g (*n*-C_{10}/LDPE = 6.3 (g/g)); PA, 500 mg; WO_x/SiO_2, 800 mg; 4A, 1.0 g. Pretreatment conditions: 480 °C; He flow (100 mL/min); 2 h. Reaction conditions: 300 °C; N_2, 30 bar; 3 h. The bars represent an average of reaction duplicates, with error bars indicating the half range. Data for the added alkane reagent/solvent (indicated in (a)) were omitted. (b) Differential molecular weight distributions of solid products from various works [18,19], including the virgin LDPE and post-reaction solid residue from alkane-metathesis (C10/LDPE) in this work (as measured by HT-GPC).
Note: Distributions from the works of Ellis *et al.* [18] and Jia *et al.* [19] were obtained by digitizing the published figures.

Detailed analysis of the solid residues for the alkane-metathesis (C10/LDPE) was performed using HT-GPC analysis (**Figure 4(b)** and **Table 3**). The significant reduction in molecular weight and dispersity (*Đ*) of LDPE demonstrates that complete conversion of the polymer occurs toward a nearly homogenous product mixture with no remaining LDPE. Two distinct populations within the measured molecular weight distributions of the products were noted: the most prominent centered around ~700 Da, corresponding to wax, and the other at ~200 Da, corresponding to mid-alkanes. Further quantification was not attempted due to the uncertainty of resolving individual peaks that were approaching the calibration limit of the GPC.

3.6 Chemical upgrading of PE via catalytic alkane metathesis reaction

The reaction conditions and results for the chemical upgrading of PE (LDPE or HDPE) via catalytic alkane metathesis reaction from two other reports [18,19] were compared to those of this work (**Figure 4(b)** and **Table 3**) to assess the relative performance of the three systems. The main difference in these three reports is the metal component of the metathesis catalyst: rhenium oxide for Ellis *et al.* and Jia *et al.* versus tungsten oxide for this work. The high volatility of the surface rhenium oxide limits the reaction temperature of this catalytic system to 175 °C and 200 °C for Jia *et al.* and Ellis *et al.*, respectively, and leads to long reaction times [18,19,21,22]. In contrast, the accessibility of a higher reaction temperature (300 °C) allowed by the thermal stability of surface tungsten oxide in this work should enhance the dehydrogenation rate and lead to a higher concentration of olefin intermediates facilitating the olefin metathesis step. In the system developed herein, the reaction required only 3 h to degrade all the polymer to molecules of interest at 300 °C, comparable to the operating temperature of other catalytic degradation reactions [4,12,16,65,66]. Our results demonstrate a notable efficiency gain relative to previous studies [18,19], whereby our reaction system required the least amount of solvent (short-chain alkane) relative to LDPE and exhibited the most significant drop in M_w and *Đ*. Specifically, our alkane metathesis (C10/LDPE) achieved a reduction in M_w of 99% and a reduction in *Đ* of over 6-fold, both in comparison to the initial LDPE (**Table 3**). The catalyst system used by Ellis *et al.* yields solid residues with two very distinct components; small hydrocarbons and polymer with a broad range of molecular weights [18]. The system used by Jia *et al.* leads to results similar to those presented here, with a product

consisting of a relatively narrow distribution of smaller molecular weights [19]. In Jia *et al.*'s case, the products have a larger M_w and $Đ$ than the results presented here [19].

Table 3. Comparison of catalytic results for chemical upgrading processes of PE via alkane metathesis in recent literature

Reference			This work	Ellis *et al.* [18]	Jia *et al.* [19]
Olefin metathesis catalyst (metal loading, wt%), quantity (g)			WO_x/SiO_2 (2), 0.8	$Re_2O_7/\gamma\text{-}Al_2O_3$ (8), 0.5	$Re_2O_7/\gamma\text{-}Al_2O_3$ (5), 0.5
(De)hydrogenation catalyst (metal loading, wt%), quantity			$Pt/\gamma\text{-}Al_2O_3$ (1.0), 0.5 g	$SnPt/\gamma\text{-}Al_2O_3$ (1.7, 0.8)[a], 0.5 g	Ir complex/$\gamma\text{-}Al_2O_3$, 4.2 µmol (Ir basis)
PE, quantity (g)			LDPE, 1.6	HDPE, 0.13	LDPE, 0.12
Short alkane, quantity (g)			*n*-decane, 9.6	*n*-pentane, 18.8	*n*-octane, 2.8
Short alkane/PE ratio (g/g)			6.0	144.5	23.4
Reaction temperature (°C)			300	200	175
Reaction time (h)			3	15	96
Molecular weight of virgin PE and wax (kDa)	Before Reaction (virgin PE)	M_n	9.1[b]	17.9[c]	5.1
		M_w	75.2[b]	52.8[c]	97.7
		$Đ$	8.3[b]	2.9[c]	17.9
	After reaction (wax)	M_n	0.68[b]	2.6[d]	1.1
		M_w	0.84[b]	14.2[d]	4.3
		$Đ$	1.2[b]	5.5[d]	4.0

[a]: Note that values given in parentheses indicate the loading of Sn and Pt, respectively.
[b]: Values were calculated considering data for molecular weights > 300 Da.
[c]: M_n, M_w, and $Đ$ were obtained by integrating the standard distribution from [67].
[d]: These values are obtained by digitizing the reported distribution and integrating for molecular weights > 500 Da (after Mark-Houwink correction [48]).

4. Conclusions

This report establishes a new alkane metathesis reaction system comprised of WO_x/SiO_2 conducted in batch mode for PE upgrading. Given the oxophilic properties of tungsten oxide, the presence of zeolites in the reaction vessel facilitates the activation of the catalyst and stabilizes active sites, which are otherwise poisoned by oxygenates generated in situ during the activation step. The pretreatment temperature of catalysts and the length of short-chain alkane are vital factors that significantly affect the catalyst's reactivity, and these parameters are under further investigation. Among other reports related to the degradation of PE using the catalytic metathesis reaction, the WO_x/SiO_2 system demonstrates a remarkable potential for the chemical upgrading of PE at short reaction times (3 h) with the lowest relative mass of solvent (the short-chain alkane) required to convert LDPE and the capacity to produce solid products of homogenous molecular weight distributions with the most significant reduction in M_w and *Đ*. Further investigation is ongoing, particularly to optimize process parameters, demonstrate catalyst regeneration, quantify metathesis kinetics, and explore other polyolefin substrates (*e.g.,* HDPE).

Appendix

List of acronyms and abbreviations

<Model reactions; olefin-metathesis/alkane-metathesis (Cx/Cy)>

Olefin-metathesis (Cx/Cy) stands for the metathesis reaction of *α*-olefin reactant of carbon number y in an *n*-alkane solvent of carbon number x. Alkane-metathesis (Cx/Cy) means the metathesis conducted between two alkane reactants of carbon number x and y; x indicates the carbon number of *n*-alkane for the short-chain alkane, which plays a role as a reactant as well as the solvent, and y indicates the carbon number of *n*-alkane for the polyethylene (PE) surrogate. The type of PE is noted instead of Cy when the polymer is added as a reactant.

- Alkane-metathesis (C7/C16): alkane metathesis between *n*-heptane and *n*-hexadecane
- Alkane-metathesis (C10/C16): alkane metathesis between *n*-decane and *n*-hexadecane
- Alkane-metathesis (C10/LDPE): alkane metathesis between *n*-decane and low-density PE (LDPE)
- Olefin-metathesis (C7/C16): olefin metathesis of 1-hexadecene in *n*-heptane

<Others>

- 1-$C_{16=}$: 1-hexadecene (1-$C_{16}H_{32}$)
- *n*-C_7: *n*-heptane (*n*-C_7H_{16})
- *n*-C_{10}: *n*-decane (*n*-$C_{10}H_{22}$)
- *n*-C_{16}: *n*-hexadecane (*n*-$C_{16}H_{34}$)
- 4A: zeolite 4A
- C.B.: carbon balance
- *Đ*: molecular weight dispersity
- GC-FID: gas chromatography-flame ionization detector
- GC-MS: gas chromatography-mass spectrometry
- HT-GPC: high-temperature gel permeation chromatography
- LDPE / HDPE: low-density polyethylene / high-density polyethylene
- M_n: number-average molecular weight
- M_w: weight-average molecular weight
- PA: platinum supported on γ-alumina
- PE: polyethylene
- S_{BET}: Brunauer–Emmett–Teller (BET) surface area
- SEM: scanning electron microscope
- V_p: total pore volume
- WO_x/SiO_2: silica-supported tungsten oxide catalyst

Acknowledgements

This work was supported as part of the Center for Plastics Innovation, an Energy Frontier Research Center funded by the U.S. Department of Energy, Office of Science, Basic Energy Sciences under Award DE-SC0021166.

References

[1] L.T.J. Korley, T.H. Epps, III, B.A. Helms, A.J. Ryan, Toward polymer upcycling-adding value and tackling circularity, Science 373 (2021) 66-69, https://doi.org/10.1126/science.abg4503

[2] R. Geyer, J.R. Jambeck, K.L. Law, Production, use, and fate of all plastics ever made, Sci. Adv. 3 (2017) e1700782, https://doi.org/10.1126/sciadv.1700782.

[3] G.W. Coates, Y.D.Y.L. Getzler, Chemical recycling to monomer for an ideal, circular polymer economy, Nat. Rev. Mater. 5 (2020) 501–516, https://doi.org/10.1038/s41578-020-0190-4

[4] B.C. Vance, P.A. Kots, C. Wang, Z.R. Hinton, C.M. Quinn, T.H. Epps, III, L.T.J. Korley, D.G. Vlachos, Single pot catalyst strategy to branched products via adhesive isomerization and hydrocracking of polyethylene over platinum tungstated zirconia, Appl. Catal. B Environ. 299 (2021) 120483, https://doi.org/10.1016/j.apcatb.2021.120483.

[5] M. Zeng, Y.H. Lee, G. Strong, A.M. Lapointe, A.L. Kocen, Z. Qu, G.W. Coates, S.L. Scott, M.M. Abu-Omar, Chemical upcycling of polyethylene to value-added α,ω-divinyl-functionalized oligomers, ACS Sustain. Chem. Eng. 9 (2021) 13926–13936, https://doi.org/10.1021/acssuschemeng.1c05272.

[6] Y. Nakaji, M. Tamura, S. Miyaoka, S. Kumagai, M. Tanji, Y. Nakagawa, T. Yoshioka, K. Tomishige, Low-temperature catalytic upgrading of waste polyolefinic plastics into liquid fuels and waxes, Appl. Catal. B Environ. 285 (2021) 119805, https://doi.org/10.1016/j.apcatb.2020.119805.

[7] H. Chen, K. Wan, Y. Zhang, Y. Wang, Waste to Wealth: Chemical recycling and chemical upcycling of waste plastics for a great future, ChemSusChem 14 (2021) 4123-4136, https://doi.org/10.1002/cssc.202100652.

[8] C. Jia, S. Xie, W. Zhang, N.N. Intan, J. Sampath, J. Pfaendtner, H. Lin, Deconstruction of high-density polyethylene into liquid hydrocarbon fuels and lubricants by hydrogenolysis over Ru catalyst, Chem Catal. 1 (2021) 253-254, https://doi.org/10.1016/j.checat.2021.04.002.

[9] S. Liu, P.A. Kots, B.C. Vance, A. Danielson, D.G. Vlachos, Plastic waste to fuels by hydrocracking at mild conditions, Sci. Adv. 7 (2021) eabf8283, https://doi.org/10.1126/sciadv.abf8283.

[10] K.L. Sanchez-Rivera, G.W. Huber, Catalytic hydrogenolysis of polyolefins into alkanes, ACS Cent. Sci. 7 (2021) 17-19, https://doi.org/10.1021/acscentsci.0c01637.

[11] A.J. Martín, C. Mondelli, S.D. Jaydev, J. Pérez-Ramírez, Catalytic processing of plastic waste on the rise, Chem 7 (2021) 1487-1533, https://doi.org/10.1016/j.chempr.2020.12.006.

[12] F. Zhang, M. Zeng, R.D. Yappert, J. Sun, Y.H. Lee, A.M. LaPointe, B. Peters, M.M. Abu-Omar, S.L. Scott, Polyethylene upcycling to long-chain alkylaromatics by tandem hydrogenolysis/aromatization, Science 370 (2020) 437–441, https://doi.org/10.1126/science.abc5441.

[13] A. Tennakoon, X. Wu, A.L. Paterson, S. Patnaik, Y. Pei, A.M. LaPointe, S.C. Ammal, R.A. Hackler, A. Heyden, I.I. Slowing, G.W. Coates, M. Delferro, B. Peters, W. Huang, A.D. Sadow, F.A. Perras, Catalytic upcycling of high-density polyethylene via a processive mechanism, Nat. Catal. 3 (2020) 893–901, https://doi.org/10.1038/s41929-020-00519-4.

[14] L.O. Mark, M.C. Cendejas, I. Hermans, The use of heterogeneous catalysis in the chemical valorization of plastic waste, ChemSusChem 13 (2020) 5808-5836, https://doi.org/10.1002/cssc.202001905.

[15] C. Wang, T. Xie, P.A. Kots, B.C. Vance, K. Yu, P. Kumar, J. Fu, S. Liu, G. Tsilomelekis, E.A. Stach, W. Zheng, D.G. Vlachos, Polyethylene hydrogenolysis at mild conditions over ruthenium on tungstated zirconia, JACS Au. 1 (2021) 1422–1434, https://doi.org/10.1021/jacsau.1c00200.

[16] G. Celik, R.M. Kennedy, R.A. Hackler, M. Ferrandon, A. Tennakoon, S. Patnaik, A.M. LaPointe, S.C. Ammal, A. Heyden, F.A. Perras, M. Pruski, S.L. Scott, K.R. Poeppelmeier, A.D. Sadow, M. Delferro, Upcycling single-use polyethylene into high-quality liquid products, ACS Cent. Sci. 5 (2019) 1795-1803, https://doi.org/10.1021/acscentsci.9b00722.

[17] J.E. Rorrer, G.T. Beckham, Y. Román, R.- Leshkov, Conversion of polyolefin waste to liquid alkanes with Ru-based catalysts under mild conditions, JACS Au. 1 (2020) 8–12, https://doi.org/10.1021/jacsau.0c00041.

[18] L.D. Ellis, S.V. Orski, G.A. Kenlaw, A.G. Norman, K.L. Beers, Y. Román-Leshkov, G.T. Beckham, Tandem heterogeneous catalysis for polyethylene depolymerization via an olefin-intermediate process, ACS Sustain. Chem. Eng. 9 (2021) 623–628, https://doi.org/10.1021/acssuschemeng.0c07612.

[19] X. Jia, C. Qin, T. Friedberger, Z. Guan, Z. Huang, Efficient and selective degradation of polyethylenes into liquid fuels and waxes under mild conditions, Sci. Adv. 2 (2016) e1501591, https://doi.org/10.1126/sciadv.1501591.

[20] S. Lwin, I.E. Wachs, Olefin metathesis by supported metal oxide catalysts, ACS Catal. 4 (2014) 2505–2520, https://doi.org/10.1021/cs500528h.

[21] F.D. Hardcastle, I.E. Wachs, J.A. Horsley, G.H. Via, The structure of surface rhenium oxide on alumina from laser raman spectroscopy and x-ray absorption near-edge spectroscopy, J. Mol. Catal. 46 (1988) 15–36, https://doi.org/10.1016/0304-5102(88)85081-8.

[22] B. Mitra, X. Gao, I.E. Wachs, A.M. Hirt, G. Deo, Characterization of supported rhenium oxide catalysts: effect of loading, support and additives, Phys. Chem. Chem. Phys. 3 (2001) 1144–1152, https://doi.org/10.1039/b007381o.

[23] R. Spronk, J.C. Mol, Regeneration of rhenium-based catalysts for the metathesis of propene, Appl. Catal. 76 (1991) 143–152, https://doi.org/10.1016/0166-9834(91)80010-T.

[24] A. Behr, U. Schüller, K. Bauer, D. Maschmeyer, K.D. Wiese, F. Nierlich, Investigations of reasons for the deactivation of rhenium oxide alumina catalyst in the metathesis of pentene-1, Appl. Catal. A Gen. 357 (2009) 34–41, https://doi.org/10.1016/j.apcata.2008.12.034.

[25] https://www.strem.com/catalog/; 0.54 $/g for tungsten powder (99.95%) and 57 $/g for rhenium powder (99.99%))

[26] J.G. Howell, Y.P. Li, A.T. Bell, Propene metathesis over supported tungsten oxide catalysts: a study of active site formation, ACS Catal. 6 (2016) 7728–7738, https://doi.org/10.1021/acscatal.6b01842.

[27] S. Lwin, Y. Li, A.I. Frenkel, I.E. Wachs, Nature of WO_x sites on SiO_2 and their molecular structure-reactivity/selectivity relationships for propylene metathesis, ACS Catal. 6 (2016) 3061–3071, https://doi.org/10.1021/acscatal.6b00389.

[28] G. Chen, M. Dong, J. Li, Z. Wu, G. Wang, Z. Qin, J. Wang, W. Fan, Self-metathesis of 1-butene to propene over SBA-15-supported WO_3, Catal. Sci. Technol. 6 (2016) 5515–5525, https://doi.org/10.1039/c6cy00248j.

[29] Y. Yun, J.R. Araujo, G. Melaet, J. Baek, B.S. Archanjo, M. Oh, A.P. Alivisatos, G.A. Somorjai, Activation of tungsten oxide for propane dehydrogenation and its high catalytic activity and selectivity, Catal. Letters 147 (2017) 622–632, https://doi.org/10.1007/s10562-016-1915-2.

[30] W. Keim, Oligomerization of ethylene to α-olefins: discovery and development of the shell higher olefin process (SHOP), Angew. Chemie - Int. Ed. 52 (2013) 12492–12496, https://doi.org/10.1002/anie.201305308.

[31] B. Reuben, H. Wittcoff, The SHOP process: an example of industrial creativity, J. Chem. Educ. 65 (1988) 605–607, https://doi.org/10.1021/ed065p605.

[32] E.F. Lutz, Shell higher olefins process, J. Chem. Educ. 63 (1986) 202–203, https://doi.org/10.1021/ed063p202.

[33] A.J. Moffat, A. Clark, M.M. Johnson, Mass transfer effects in the olefin disproportionation reaction: I. Promoter concentration and temperature effects for propylene on WO_3-silica catalysts, J. Catal. 22 (1971) 379–388, https://doi.org/10.1016/0021-9517(71)90210-7.

[34] T. Takkawatakarn, K. Suriye, B. Jongsomjit, J. Panpranot, P. Praserthdam, Influence of acidity on the performance of silica supported tungsten oxide catalysts assessed by in situ and Operando DRIFTS, Catal. Today 358 (2020) 345-353, https://doi.org/10.1016/j.cattod.2019.08.062.

[35] C. van Schalkwyk, A. Spamer, D.J. Moodley, T. Dube, J. Reynhardt, J.M. Botha, Application of a WO_3/SiO_2 catalyst in an industrial environment: part I, Appl. Catal. A Gen. 255 (2003) 121–131, https://doi.org/10.1016/S0926-860X(03)00534-9.

[36] A. Spamer, T.I. Dube, D.J. Moodley, C. van Schalkwyk, J.M. Botha, Application of a WO_3/SiO_2 catalyst in an industrial environment: Part II, Appl. Catal. A Gen. 255 (2003) 133–142, https://doi.org/10.1016/S0926-860X(03)00535-0.

[37] S. Watmanee, K. Suriye, P. Praserthdam, J. Panpranot, Formation of isolated tungstate sites on hierarchical structured SiO_2- and HY zeolite-supported WO_x catalysts for propene metathesis, J. Catal. 376 (2019) 150–160, https://doi.org/10.1016/j.jcat.2019.07.001.

[38] S. Boonpai, K. Suriye, B. Jongsomjit, J. Panpranot, P. Praserthdam, Hydrogen activated WO_x-supported catalysts for Lewis acid transformation to Bronsted acid observed by in situ DRIFTS of adsorbed ammonia: effect of different supports on the Lewis acid transformation, Catal. Today 358 (2020) 370-386, https://doi.org/10.1016/j.cattod.2019.06.073.

[39] H. Liu, K. Tao, H. Yu, C. Zhou, Z. Ma, D. Mao, S. Zhou, Effect of pretreatment gases on the performance of WO_3/SiO_2 catalysts in the metathesis of 1-butene and ethene to propene, Comptes Rendus Chim. 18 (2015) 644–653, https://doi.org/10.1016/j.crci.2014.11.008.

[40] R. Thomas, J.A. Moulijn, V.H.J. De Beer, J. Medema, Structure/metathesis activity relations of silica supported molybdenum and tungsten oxide, J. Mol. Catal. 8 (1980) 161–174, https://doi.org/10.1016/0304-5102(80)87015-5.

[41] A. Spamer, T.I. Dube, D.J. Moodley, C. van Schalkwyk, J.M. Botha, The reduction of isomerisation activity on a WO_3/SiO_2 metathesis catalyst, Appl. Catal. A Gen. 255 (2003) 153–167, https://doi.org/10.1016/S0926-860X(03)00537-4.

[42] K. Gayapan, S. Sripinun, J. Panpranot, P. Praserthdam, S. Assabumrungrat, Effect of pretreatment atmosphere of WO_x/SiO_2 catalysts on metathesis of ethylene and 2-butene to propylene, RSC Adv. 8 (2018) 11693–11704, https://doi.org/10.1039/c8ra01093e.

[43] K. Gayapan, S. Sripinun, J. Panpranot, P. Praserthdam, S. Assabumrungrat, Effects of calcination and pretreatment temperatures on the catalytic activity and stability of H_2-treated WO_3/SiO_2 catalysts in metathesis of ethylene and 2-butene, RSC Adv. 8 (2018) 28555–28568, https://doi.org/10.1039/c8ra04949a.

[44] N. Popoff, E. Mazoyer, J. Pelletier, R.M. Gauvin, M. Taoufik, Expanding the scope of metathesis: a survey of polyfunctional, single-site supported tungsten systems for hydrocarbon valorization, Chem. Soc. Rev. 42 (2013) 9035–9054, https://doi.org/10.1039/c3cs60115c.

[45] R. L. Burnett, T. R. Hughes, Mechanism and poisoning of the molecular redistribution reaction of alkanes with dual-functional catalysts system, J. Catal. 31 (1973) 55-64, https://doi.org/10.1016/0021-9517(73)90270-4.

[46] C.Y. Chen, D.J. O'Rear, P. Leung, Molecular redistribution and molecular averaging: disproportionation of paraffins via bifunctional catalysis, Top. Catal. 55 (2012) 1344–1361, https://doi.org/10.1007/s11244-012-9910-3.

[47] J.C. Mol, Industrial applications of olefin metathesis, J. Mol. Catal. A Chem. 213 (2004) 39–45, https://doi.org/10.1016/j.molcata.2003.10.049.

[48] ASTM D6474-20, Standard test method for determining molecular weight distribution and molecular weight averages of polyolefins by high temperature gel permeation chromatography, ASTM International, West Conshohocken, PA, (2020), www.astm.org.

[49] V. Mougel, K.W. Chan, G. Siddiqi, K. Kawakita, H. Nagae, H. Tsurugi, K. Mashima, O. Safonova, C. Copéret, Low temperature activation of supported metathesis catalysts by organosilicon reducing agents, ACS Cent. Sci. 2 (2016) 569–576, https://doi.org/10.1021/acscentsci.6b00176.

[50] N. Morlanés, S.G. Kavitake, D.C. Rosenfeld, J.M. Basset, Alkane cross-metathesis reaction between light and heavy linear alkanes, on a silica supported well-defined single-site catalyst, ACS Catal. 9 (2019) 1274–1282, https://doi.org/10.1021/acscatal.8b02472.

[51] D.S. Kim, M. Ostromecki, I.E. Wachs, Surface structures of supported tungsten oxide catalysts under dehydrated conditions, J. Mol. Catal. A Chem. 106 (1996) 93–102. https://doi.org/10.1016/1381-1169(95)00186-7.

[52] E.I. Ross-Medgaarden, I.E. Wachs, Structural determination of bulk and surface tungsten oxides with UV-vis diffuse reflectance spectroscopy and raman spectroscopy, J. Phys. Chem. C. 111 (2007) 15089–15099. https://doi.org/10.1021/jp074219c.

[53] W. Limsangkass, P. Praserthdam, S. Phatanasri, J. Panpranot, S. Chaemchuen, W. Jareewatchara, S. Kunjara Na Ayudhya, K. Suriye, Influence of micro- and nano-sized SiO_2 excess support on the metathesis of ethylene and trans-2-butene to propylene over silica-supported tungsten catalysts, React. Kinet. Mech. Catal. 113 (2014) 225–240, https://doi.org/10.1007/s11144-014-0724-0.

[54] S. Lwin, I.E. Wachs, Catalyst activation and kinetics for propylene metathesis by supported WO_x/SiO_2 catalysts, ACS Catal. 7 (2017) 573–580, https://doi.org/10.1021/acscatal.6b03097.

[55] M. Ghodhbene, F. Bougie, P. Fongarland, M.C. Iliuta, Hydrophilic zeolite sorbents for In-situ water removal in high temperature processes, Can. J. Chem. Eng. 95 (2017) 1842–1849, https://doi.org/10.1002/cjce.22877.

[56] E. Jaramillo, M. Chandross, Adsorption of small molecules in LTA zeolites. 1. NH_3, CO_2, and H_2O in zeolite 4A, J. Phys. Chem. B 108 (2004) 20155-20159, https://doi.org/10.1021/jp048078f.

[57] A.G. Basrur, S.R. Patwardhan, S.N. Was, Propene metathesis over silica-supported tungsten oxide catalyst-catalyst induction mechanism, J. Catal. 127 (1991) 86–95, https://doi.org/10.1016/0021-9517(91)90211-L.

[58] J. Song, Z.F. Huang, L. Pan, J.J. Zou, X. Zhang, L. Wang, Oxygen-deficient tungsten oxide as versatile and efficient hydrogenation catalyst, ACS Catal. 5 (2015) 6594–6599, https://doi.org/10.1021/acscatal.5b01522.

[59] J.J.H.B. Sattler, J. Ruiz-Martinez, E. Santillan-Jimenez, B.M. Weckhuysen, Catalytic dehydrogenation of light alkanes on metals and metal oxides, Chem. Rev. 114 (2014) 10613–10653, https://doi.org/10.1021/cr5002436.

[60] J.W. Park, J.H. Kim, G. Seo, The effect of pore shape on the catalytic performance of zeolites in the liquid-phase degradation of HDPE, Polym. Degrad. Stab. 76 (2002) 495–501, https://doi.org/10.1016/S0141-3910(02)00059-9.

[61] L. Shuai, J. Luterbacher, Organic solvent effects in biomass conversion reactions, ChemSusChem 9 (2016) 133–155, https://doi.org/10.1002/CSSC.201501148.

[62] William E. Acree, Jr., James S. Chickos, "Phase transition enthalpy measurements of organic and organometallic compounds" in NIST Chemistry WebBook, NIST Standard Reference Database Number 69, Eds. P.J. Linstrom and W.G. Mallard, National Institute of Standards and Technology, Gaithersburg MD, 20899, https://doi.org/10.18434/T4D303, (retrieved November 12, 2021).

[63] X. Ding, H. Zhu, H. Ren, D. Liu, Z. Yu, N. Shi, W. Guo, Adsorption and dehydrogenation of C_2-C_6*n*-alkanes over a Pt catalyst: a theoretical study on the size effects of alkane molecules and Pt substrates, Phys. Chem. Chem. Phys. 22 (2020) 21835–21843, https://doi.org/10.1039/d0cp03194a.

[62] Y.H. Lin, M.H. Yang, T.F. Yeh, M.D. Ger, Catalytic degradation of high density polyethylene over mesoporous and microporous catalysts in a fluidised-bed reactor, Polym. Degrad. Stab. 86 (2004) 121–128, https://doi.org/10.1016/j.polymdegradstab.2004.02.015.

[63] P.A. Kots, S. Liu, B.C. Vance, C. Wang, J.D. Sheehan, D.G. Vlachos, Polypropylene plastic waste conversion to lubricants over Ru/TiO_2 catalysts, ACS Catal. 11 (2021) 8104–8115, https://doi.org/10.1021/acscatal.1c00874.

[64] D.P. Serrano, J. Aguado, J.M. Escola, Developing advanced catalysts for the conversion of polyolefinic waste plastics into fuels and chemicals, ACS Catal. 2 (2012) 1924–1941, https://doi.org/10.1021/cs3003403.

[65] C.A.J. Hoeve, H.L. Wagner, P.H. Verdier, The characterization of linear polyethylene SRM 1475. I. introduction, J. Res. Natl. Bur. Stand. Sect. A. Phys. Chem. 76A (1972) 137-140, https://doi.org/10.6028/jres.076a.014.

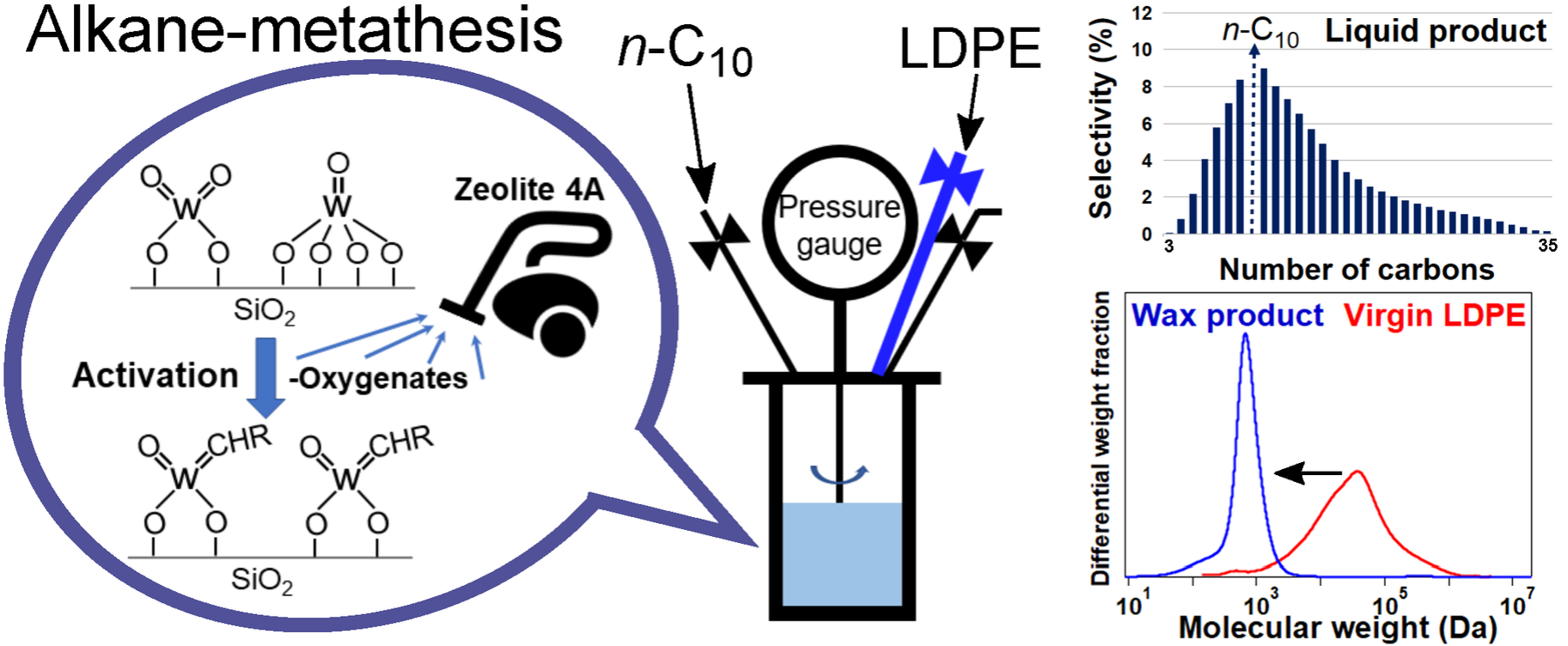
Alkane-metathesis
n-C10
LDPE
Zeolite 4A
Pressure gauge
SiO2
Activation
-Oxygenates
CHR
SiO2
Selectivity (%)
n-C10
Liquid product
Number of carbons
Wax product
Virgin LDPE
Differential weight fraction
Molecular weight (Da)